NASA/TM—2006-214387

Undercutting Studies of Protected Kapton® H Exposed to In-Space and Ground-Based Atomic Oxygen

Aaron Snyder and Bruce A. Banks
Glenn Research Center, Cleveland, Ohio

Deborah L. Waters
QSS Group, Inc., Cleveland, Ohio

August 2006

NASA STI Program . . . in Profile

Since its founding, NASA has been dedicated to the advancement of aeronautics and space science. The NASA Scientific and Technical Information (STI) program plays a key part in helping NASA maintain this important role.

The NASA STI Program operates under the auspices of the Agency Chief Information Officer. It collects, organizes, provides for archiving, and disseminates NASA's STI. The NASA STI program provides access to the NASA Aeronautics and Space Database and its public interface, the NASA Technical Reports Server, thus providing one of the largest collections of aeronautical and space science STI in the world. Results are published in both non-NASA channels and by NASA in the NASA STI Report Series, which includes the following report types:

- TECHNICAL PUBLICATION. Reports of completed research or a major significant phase of research that present the results of NASA programs and include extensive data or theoretical analysis. Includes compilations of significant scientific and technical data and information deemed to be of continuing reference value. NASA counterpart of peer-reviewed formal professional papers but has less stringent limitations on manuscript length and extent of graphic presentations.

- TECHNICAL MEMORANDUM. Scientific and technical findings that are preliminary or of specialized interest, e.g., quick release reports, working papers, and bibliographies that contain minimal annotation. Does not contain extensive analysis.

- CONTRACTOR REPORT. Scientific and technical findings by NASA-sponsored contractors and grantees.

- CONFERENCE PUBLICATION. Collected papers from scientific and technical conferences, symposia, seminars, or other meetings sponsored or cosponsored by NASA.

- SPECIAL PUBLICATION. Scientific, technical, or historical information from NASA programs, projects, and missions, often concerned with subjects having substantial public interest.

- TECHNICAL TRANSLATION. English-language translations of foreign scientific and technical material pertinent to NASA's mission.

Specialized services also include creating custom thesauri, building customized databases, organizing and publishing research results.

For more information about the NASA STI program, see the following:

- Access the NASA STI program home page at *http://www.sti.nasa.gov*

- E-mail your question via the Internet to *help@sti.nasa.gov*

- Fax your question to the NASA STI Help Desk at 301–621–0134

- Telephone the NASA STI Help Desk at 301–621–0390

- Write to:
  NASA STI Help Desk
  NASA Center for AeroSpace Information
  7121 Standard Drive
  Hanover, MD 21076–1320

NASA/TM—2006-214387

Undercutting Studies of Protected Kapton® H Exposed to In-Space and Ground-Based Atomic Oxygen

Aaron Snyder and Bruce A. Banks
Glenn Research Center, Cleveland, Ohio

Deborah L. Waters
QSS Group, Inc., Cleveland, Ohio

Prepared for the
10th International Symposium on Materials in a Space Environment (ISMSE)
cosponsored by the ONERA, CNES, and ESA
Collioure, France, June 19–23, 2006

National Aeronautics and
Space Administration

Glenn Research Center
Cleveland, Ohio 44135

August 2006

Level of Review: This material has been technically reviewed by technical management.

Available from

NASA Center for Aerospace Information
7121 Standard Drive
Hanover, MD 21076–1320

National Technical Information Service
5285 Port Royal Road
Springfield, VA 22161

Available electronically at http://gltrs.grc.nasa.gov

Undercutting Studies of Protected Kapton® H Exposed to In-Space and Ground-Based Atomic Oxygen

Aaron Snyder and Bruce A. Banks
National Aeronautics and Space Administration
Glenn Research Center
Cleveland, Ohio 44135

Deborah L. Waters
QSS Group, Inc.
Cleveland, Ohio 44135

Abstract

This study is part of a Materials International Space Station Experiment (MISSE) sequence to characterize the performance of prospective spacecraft materials when subjected to the synergistic effects of the space environment. Atomic oxygen (AO) is the most prevalent species in low earth orbit (LEO). In this environment AO is mainly responsible for the erosion of hydrocarbons and halocarbon polymers. The AO erosion rates of Kapton (DuPont) H are known and well documented. Hence, it is customary to compare the AO erosion yields of candidate materials to the commonly accepted standard of this polyimide. The purpose of this study was to provide characterization of AO degradation of SiO_x protected Kapton H film, which was subject during MISSE 2 to undercutting erosion beneath microscopic defects in the protective film, and compare the degradation resulting from hyperthermal ram (~4.5 eV) LEO AO to the degradation resulting from exposure to thermal ground-based (~0.04 eV) AO.

1. Introduction

Affordable routine access to space requires the testing and development of new generations of materials and material technologies. New affordable materials are the enablers for advanced reusable launch systems and advanced spacecraft systems including optics, sensors, electronics, power, coatings, structural materials and environmental protection. In-situ space testing is an essential part of the development processes for new generations of space materials because terrestrial laboratory facilities cannot simulate the synergistic effects of the combined space environments.

This study is part of a Materials International Space Station Experiment (MISSE) sequence to characterize the performance of prospective spacecraft materials when subjected to the long term synergistic effects of the space environment (refs. 1 and 2). The present work is the exploratory phase of a two phase experiment conducted by researchers at the National Aeronautics and Space Administration's (NASA) Glenn Research Center (GRC). The work reported herein is part of MISSE 2, which is sponsored by the Materials Laboratory at the Air Force Research Laboratory, and NASA. It utilizes Passive Experiment Containers (PECs) developed by Langley Research Center (LaRC) and first used for ISS Phase I Risk Mitigation Experiments on Mir.

Knowing the erosion yields of a wide variety of polymers subject to the LEO environment is of vital importance in predicting the durability and lifetime of essential spacecraft components. AO is the principle species in LEO. Hyperthermal (~4.5 eV) AO is mainly responsible for the erosion of hydrocarbons and halocarbon polymers. The rates of erosion are appreciable, such that depths of tens of micrometers are capable of being removed within months. The rate of erosion depends on the chemical structure of the polymer. The particular polyimide Kapton H has a number of characteristics that make it a suitable choice for both space and terrestrial applications; e.g., it serves as a blanket material in solar arrays. The AO erosion rates of Kapton H are known and well documented. Hence, it is customary to compare the AO erosion yields of various candidate materials, measured in volume of material oxidized per incident AO-atom, to the commonly accepted standard of the polyimide
Kapton H.

To protect polymers from extreme degradation, they are often coated with very thin films of erosion-resistant material such as SiO_x, where the numerical value of x is approximately 2. However, scratch, crack or pin-window defects in the coatings exist that allow the base polymer to be attacked. These defects may arise during coating application, or later due to handling and other mechanical stresses, or via micro-meteoroid and debris strikes while in service. Undercutting erosion begins at the defect site. With continued AO exposure, the erosion zone spreads beneath the protective coating to greater depths and widths proceeding through the substrate in an "undercutting" fashion. Figure 1 shows a picture obtained using a scanning electron microscope of a pin-window defect above an undercutting site.

The shape of undercut erosion depends upon the material, defect type, and distribution, energy, and arrival direction of the incident AO. Over time the erosion can progress to the point that the substrate loses it mechanical integrity thus jeopardizing component functionality. Because protected Kapton is so widely used, it is essential to be able to predict its AO durability in the LEO environment.

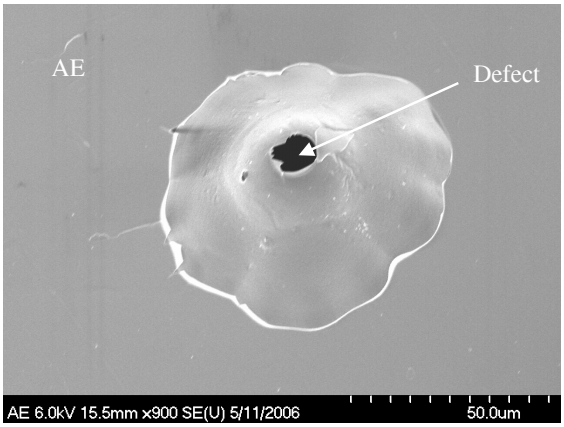

Figure 1.—SEM view of defect in SiO_x coating.

LEO test allocations such as MISSE 2 are limited, thus it is highly desirable to develop a correlation between the in-space AO erosion characteristics of materials and ground-based AO erosion characteristics to be able to predict in-space behavior based on ground laboratory test results. Although it is most convenient to use isotropic thermal energy RF plasma ashers to assess AO durability, the results can be misleading in part because the relative erosion rates at thermal energies (~0.04 eV) differ from LEO ram AO energies (~4.5 eV). Furthermore, the undercutting process is influenced by the geometry of the undercut cavity, which changes shape with AO fluence. The AO erosion varies with cavity shape due to its dependence on the distribution and energy of AO within the cavity. The interdependence of cavity shape and growth with fluence complicates the undercutting process beyond the consideration of initial AO energy distributions of in-space and ground-based AO.

To help interpret and predict the undercutting process computational codes as in (refs. 3 to 5) are often employed that simulate the undercutting erosion taking place beneath defects (ref. 6) in the protective film. These computational codes have been developed to various levels of sophistication. The more sophisticated codes rely on Monte-Carlo statistics, advanced ray-tracing techniques, and decision based rules controlling the actions of individual computational atoms acting as surrogates for real AO atoms. Although the number of parameters used varies widely based on the simulation method, the capability of a simulation to realistically predict AO undercutting erosion largely depends on adequately specifying the program parameters that control the erosion and the AO extinction rates at the various surface components of the undercut cavity.

The purpose of this experimental study is to compare the erosion characteristics between in-space and ground-based AO exposure of protected Kapton and provide data whereby in-space durability can be predicted based on ground-based results. This exploratory phase of the experiment should hopefully serve to provide direction for the second phase planned as part of a future MISSE experiment.

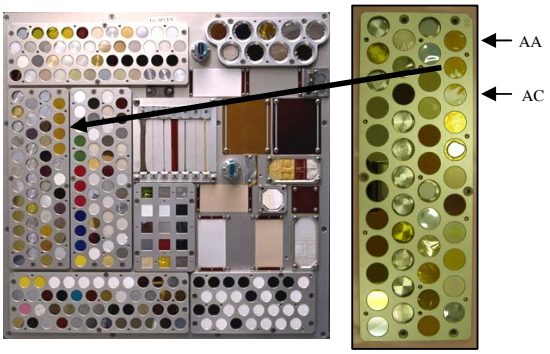

Figure 2.—MISSE 2 (PEC 2) Tray 1 with enlarged view of holder 2-E6 showing samples AA and AC.

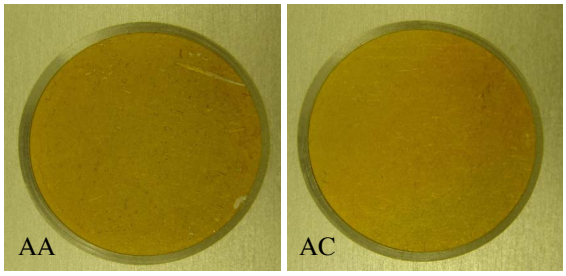

Figure 3.—Post-flight samples AA and AC.

To accomplish this goal an experimental procedure was followed as outlined here. Identical samples were cut from a common piece of SiO_x protected Kapton H and exposed to a differing series of AO environments. Four of these samples were exposed concurrently in a thermal-energy RF plasma asher to effective AO fluence levels (4.03×10^{21} atoms/cm^2) corresponding to nearly two-years of in-space ram AO exposure. Sample mass loss was measured and numerous undercutting sites were identified and analyzed. Two samples (among a diversified tray of polymer samples, see fig. 2) of protected Kapton H were transported to the International Space Station (ISS) attached to the exterior of the ISS during (August 16, 2001) the STS 105 Shuttle mission. The materials were retrieved (July 30, 2005) during the STS–114 Shuttle mission. One of these samples (AA) was from the pre-exposed set while the other sample (AC) was pristine. Aboard the ISS the samples were exposed to ram AO fluence levels (8.51×10^{21} atoms/cm^2) (ref. 2) corresponding to nearly four-years of in-space ram AO exposure. Upon retrieval the two flight samples (fig. 3) together with a non-flight asher-exposed sample (AE) were inspected, weighed for mass loss, and analyzed extensively using optical and electron microscopy in order to characterize the effects of AO exposure. This paper presents and discusses the preliminary analysis of the in-space (hyperthermal) AO erosion and the ground-based (thermal) AO erosion of Kapton H.

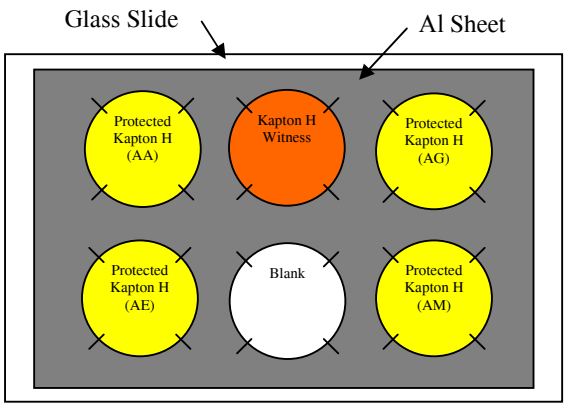

Figure 4.—Plasma asher sample and witness layout.

2. Experimental

For ground-based AO this study used a 13.56-MHz SPI Plasma Prep-II asher operated with air. This type of asher produces AO by the use of a low pressure, radio-frequency induced, gaseous discharge. The optical measurements were made using an Olympus SZH microscope and a Keyence VHX Microscope. The Olympus microscope translation stage is equipped with a precision xy-positioner. Illumination from below a sample placed in the Olympus microscope enabled undercutting sites to be viewed over a magnification range of approximately 15 to 100x. The Keyence microscope package contains sophisticated software, which was used to obtain high quality depth composition, depth profiles, area measurement, and three-dimensional images over a range of magnification from 500x to 5000x. After sputter coating the samples with a thin (~7.5 nm) layer of Pt used to prevent excessive accumulation of electrostatic charge, a Hitachi II SEM that could resolve small defects in the coating was used to obtain numerous higher magnification (up to 20,000x) micrographs of undercutting sites.

The Kapton H samples were cut from a sheet of 0.0254-mm thickness Sheldalh-IP-701764, covered on both faces with 0.13 μm of SiO_x. Prior to weighing, all samples were stored in a vacuum desiccator at pressures between 7 to 10 Pa. Samples were weighed using a Mettler M3 microbalance. Following vacuum desiccation and initial weighing, four flight-candidate samples were subjected concurrently to four plasma-asher AO exposure sessions. Each session consisted of the following procedures: (1) 48-hour asher-exposure interval accompanied by a Kapton H witness coupon for determination of effective fluence; (2) individual sample weighing for mass-loss determination; and (3) optical microscopy to analyze undercutting size. The ashed samples were placed on a glass slide and held down by wire spiders connected to the periphery of the apertures in the thin aluminum holder plate, see fig. 4. During LEO exposure the in-flight samples resided in the holder 2–E6 of PEC 2 tray 1 in positions 1 and 3 as shown in figure 2. The nominal aperture diameter of 2.064 cm provided an exposure area of 0.339 cm^2 for each flight sample.

To place the sample mass loss on an equivalent basis, mass loss comparison was based on the erosion area available to an in-space sample. This meant an adjustment was needed for the mass loss from asher exposure since, in this case, all surfaces of a sample could contribute to the mass loss. To make this adjustment, an auxiliary plasma-asher experiment was conducted to determine the fractional mass losses attributable to the following sample surfaces: (1) the fully exposed upper side, (2) the lower side facing the glass plate, and (3) to the unprotected periphery. The fractional mass losses for the three given areas were determined to be approximately 0.31, 0.68, and 0.006, respectively.

3. Results and Discussion

This section begins by discussing the results for sample mass loss as a function of AO exposure. This is followed by presenting the analysis based on percent coverage of sample surface due to undercutting area. Finally, analysis obtained using optical and electron microscopy of individual undercutting sites are presented and discussed.

3.1 Mass Loss

Mass loss results are summarized in table I for the portions of exposure to thermal and hyperthermal AO; i.e., the mass-loss and fluence given in the table are not cumulative. The rates of mass loss for the various stages of exposure are also given. Figure 5 illustrates these results by showing the fractional mass remaining as a function of AO fluence. The rate of mass loss for sample AA that occurred during exposure to thermal AO is seen to be about twice the rate that occurred during exposure to LEO hyperthermal AO. This is not unexpected since energy accommodation for hyperthermal AO is significantly greater for those atoms surviving initial impact than is the case for thermal AO. Since the probability of AO to erode diminishes rapidly with increasing energy, collisions within the cavity cause surviving hyperthermal AO to become much less effective as an eroding agent as accommodation proceeds via surface interactions.

The comparison of the mass loss due to in-space exposure between sample AA and AC reveal that the rate of mass loss is six times greater when pre-exposed to asher AO. This factor is much greater than the thermal sample-to-sample variation, which is less than 15 percent. It is known that large amounts of exposure to AO allow tearing or rolling up of the SiO_x at defect sites due to loss of mechanical support arising from depletion of the underlying polymer. Moreover, the isotropic distribution of asher AO enables AO incidence to occur over all hemispherical angles, which could "enable" certain types of defect sites due to loss of adjacent polymer material. This would be the case for contiguous but frangible sections of SiO_x held

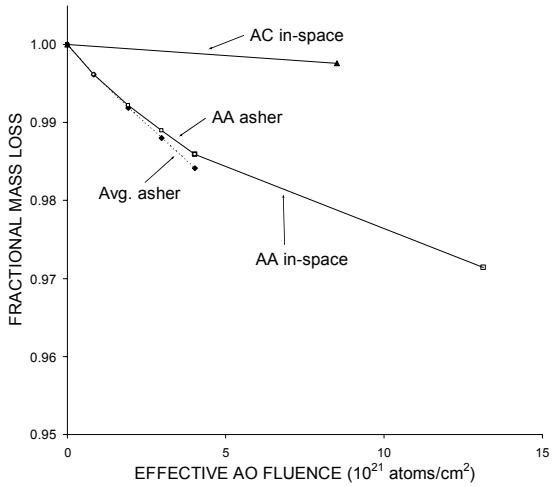

Figure 5.—Relative sample mass as a function of AO exposure.

together by the substrate. Many of these sites may hold up under "directed beam" exposure as in the case of hyperthermal AO, but such a loose protective umbrella may not withstand exposure to isotropic AO. Perhaps small to moderate levels of AO exposure cause microscopic tears to occur enhancing the undercutting process. This would explain the increased mass loss rate for the pre-exposed case. Another possible explanation for the difference in rates is if, for the pre-exposed case, thermal accommodation of hyperthermal AO is moderated sufficiently due to advantageous cavity wall composition, then increased erosion through effective trapping of persistently energetic AO could occur. Conjectures such as the above are often best examined using computational simulations, which allow parameters such as extinction coefficients to be assigned separately for individual components, such as for the SiO_x and polymer cavity surfaces.

3.2 Surface Coverage Using Optical Microscopy

Figure 6 contains typical pictures of undercutting areas for samples AA, AE, and AC and shown in this order from top to bottom. These images were taken using the Keyence microscope at a magnification of 500x. Each image covers an area of 0.25 mm^2. Based on these pictures, it is clear that sample AC experienced much less undercutting than either sample AA or AE. Using software available with the Keyence microscope, planimeter analysis was made to determine the percentage of total surface comprised by undercutting area. For each of the above samples, 16 randomly chosen locations similar to those shown in figure 6 were surveyed. The results for the coverage are as follows: 5.3, 2.3, and 0.2 percent for sample AA, AE, AC, respectively. These are approximately in the ratios 29:12:1, respectively. These percentages are inline qualitatively with the mass loss analysis presented in table I.

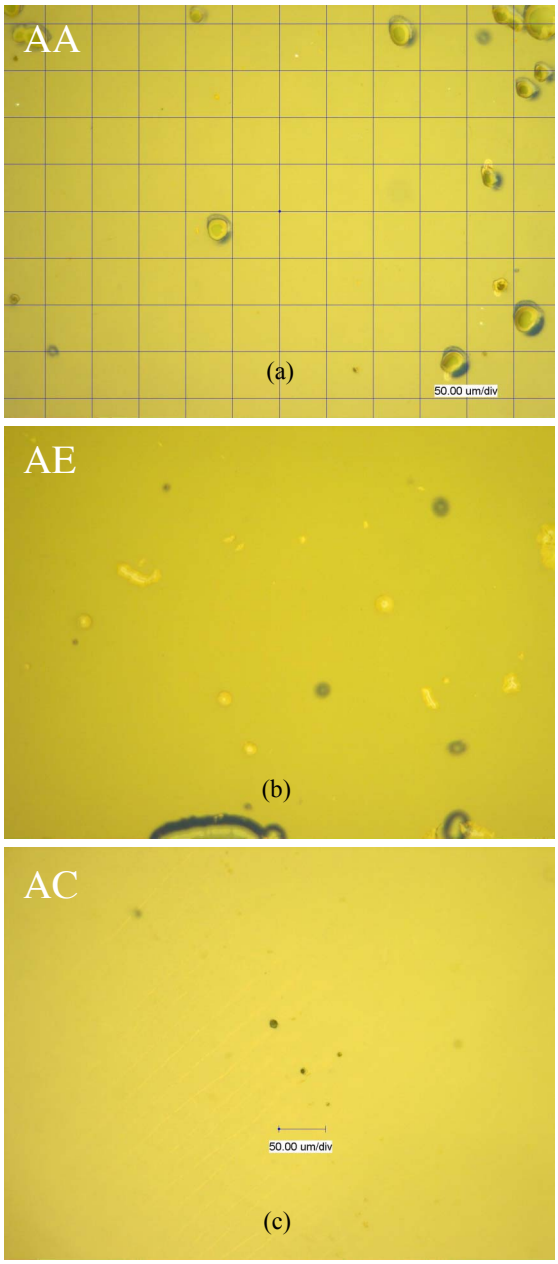

Figure 6.—Typical undercutting densities for various AO exposures: (a) asher followed by in-space, (b) asher, and (c) in-space.

TABLE I.—SUMMARY OF MASS LOSS AND AO EXPOSURE

AO source	Plasma asher (Thermal)		In-space (Hyperthermal)	
Sample	Four-sample average	AA	AA	AC
AO fluence, F atom/cm^2	4.0E+21	4.0E+21	8.5E+21	8.5E+21
Pristine mass, mg	18.717	18.548	18.548	18.412
Mass loss Δm, mg	0.297 ±0.038	0.262	0.269	0.045
Δm/F, mg·cm^2/atom	7.4E–223	6.5E–223	3.0E–23	5.0E–224
Δm/F ratios	14	12	5.5	1

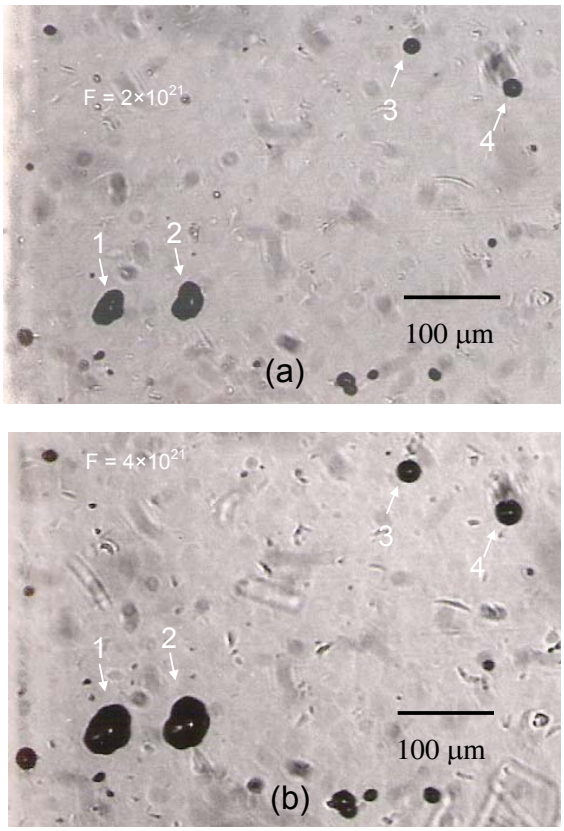

Figure 7.—Size of sample AA sites (1 to 4) exposed to asher AO before flight for (a): F = 2×10^{21} atom/cm^2 and (b): F = 4×10^{21} atom/cm^2.

3.2 Site Analysis Using Microscopy

Optical microscopy is a valuable tool in the study of undercutting of thin films. Recording of cavity silhouette dimensions was made using the Olympus microscope with illumination from below the sample. Prior to flight only the Olympus microscope with an attached camera providing Polaroid images was available. After retrieval the Keyence microscope became available. The analysis of different site locations based on optical and electron microscopy is now presented.

After each pre-flight ashing session, several site locations for each sample were recorded using the Olympus microscope. Figure 7 shows cropped images taken of sample AA (100x magnification) after sufficient undercutting occurred to enable visual observation. Polaroid images taken after the second ashing session at a cumulative fluence of F = 2×10^{21} atoms/cm^2 are shown and labeled in figure 7(a). This is the first session for which individual undercutting sites were identified. The larger pair of sites is separated in distance by about 85 µm and the smaller pair by about 125 µm. These same sites are shown in figure 7(b).

The delta fluence of 2×10^{21} atom/cm^2 resulted in an increase in cavity width of approximately 10 µm for both pairs of sites. These two pairs of undercuttings were also examined during post-retrieval analysis.

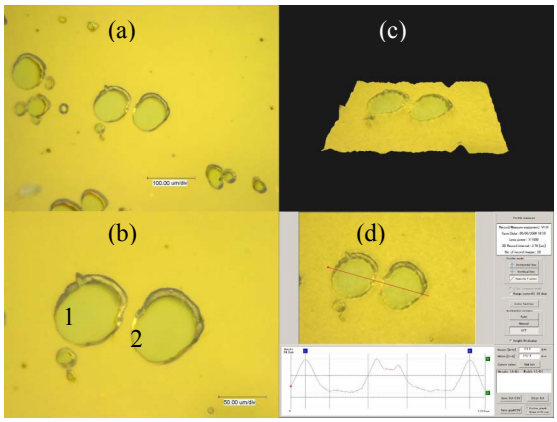

Figure 8.—Post-flight views of sites 1 and 2 on sample AA using Keyence microscope before removal of SiO_x coating.

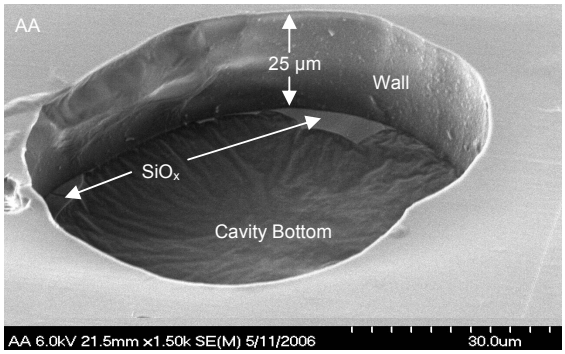

Figure 9.—SEM post-flight micrograph of site 2 of sample AA after removal of SiO_x layer and application of Pt.

Figure 8 shows a ensemble of images obtained using the Keyence microscope which allowed higher magnification of the pair of larger sites (1 and 2). Figure 8(a) shows site pair 1 and 2 at a magnification of 500x before the SiO_x film was removed from this portion of the sample. The pair enlarged in concert from an average width of approximately 50 µm to an average width of about 70 µm due to in-flight exposure to 8.5×10^{21} atom/cm^2 of hyperthermal AO. Figure 8(b) shows the pair at a magnification of 1000x. The Keyence software package includes a three-dimensional image-construction feature, which allows viewing from any perspective as shown in figure 8(c). Depth profiling is also provided along an arbitrarily drawn line as shown in figure 8(d). The profile provided indicates a depth of 24.4 µm, which closely approximates the nominal 25.4 µm film thickness. Somewhat by coincidence the same large pair (1 and 2) of sites was examined using the SEM. By peeling off the protective coating using clear commercial tape and coating a portion of the sample with a thin Pt layer, it was analyzed using the SEM. Figure 9 shows an SEM picture taken at a 45° angle showing portions of the bottom and side wall of site 2. This view (rotated ~180° w.r.t. figures 7 and 8) indicates that the cavity wall is steeply sloped. Distinct demarcations exist around the lower periphery allowing identification of the wall edge and cavity bottom, which is now

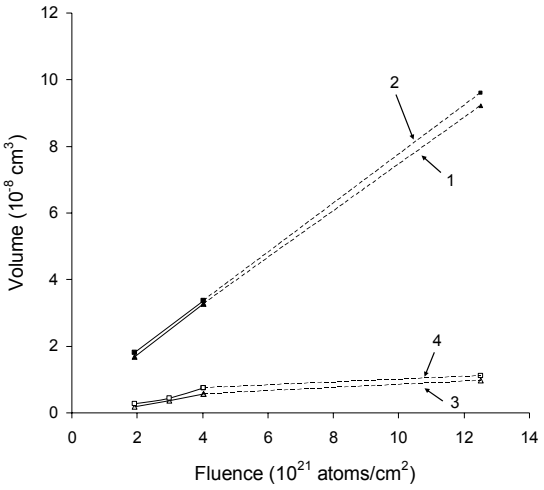

Figure 10.—Undercutting volume as a function of AO fluence (asher: solid lines, in-space: dotted lines) for sites: pair 1 to 2 and pair 3 to 4 on sample AA.

comprised of black carbon mounting tape and remnants of the lower SiO_x protective coating. Taking into account the viewing angle, the wall height was measured as 25 ± 1 μm.

An additional post-flight analysis was made of both pairs of sites (1 to 2 and 3 to 4) using the Keyence and Olympus microscopes. Based on this analysis together with a spherically-shaped geometric model as in reference 7 to calculate volume, an estimate on the evolution of cavity volume as a function of AO fluence can be made. Figure 10 presents this evolvement. In this figure, the asher portion of exposure is denoted by solid lines and the in-space exposure is denoted by dashed lines. The instep growth seen for a given undercutting pair indicates that no significant anomalous effects occurred, such as tearing of the protective film leading to an abrupt solitary enlargement of defect size (ref. 8). This suggests that any changes to these undercutting sites were from common processes such as graduated enlargement or localized sagging or uplifting of the protective film brought about by stress-relieving shifts needed to accommodate loss of adjacent polymer substrate. For both sets of undercuttings, the rate of growth is less for hyperthermal AO exposure. This result supports the mass loss results given in table I and presented in figure 5 that show fractional mass decreased at about half the rate for sample AA during exposure to hyperthermal as compared to thermal AO. Although the change in slope occurring at the thermal-to-hyperthermal juncture is greater for the smaller sites compared to the change in slope of the larger sites, supporting data accumulated from many sites would be needed before a conclusion could be made that this is a general trend.

The discussion proceeds to the analysis of sample AC, which was exposed to hyperthermal AO only. As seen by comparing the example of in-space only exposure presented in figure 6(c) to the asher-exposed cases presented in figure 6(a) and (b), the in-space undercutting sites are much smaller than the ashed

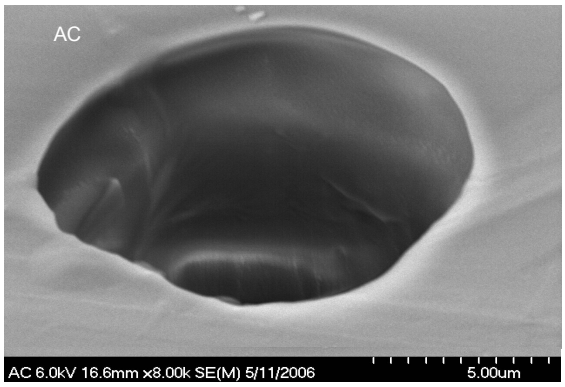

Figure 11.—Post-flight SEM micrograph of site on sample AC.

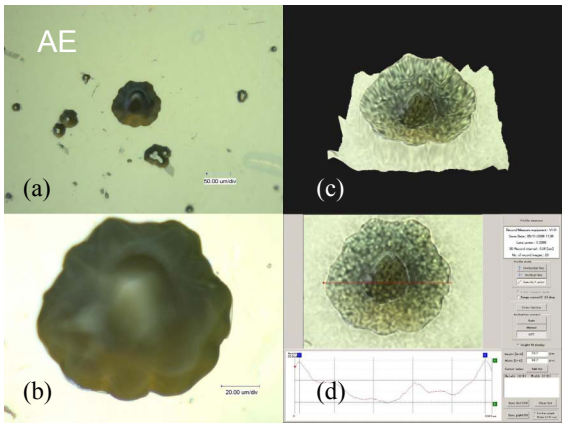

Figure 12.—Post-flight views of typical site on sample AE using Keyence microscope after removal of SiO_x protective coating and application of Pt coating.

sample sites. In general the observed in-spaced undercutting widths of sample AC are between 5 and 15 μm. In contrast, for the asher only undercutting of sample AE, widths up to 50 μm are common and many exceed this as shown in a later example. Figure 11 shows an in-space undercutting site on sample AC using the SEM with the sample inclined at 45°. The undercutting width is 12.5 μm. The sample tilt of 45° is too steep to reveal the full depth of the cavity, however, based on profile analysis of similar sites performed using the Keyence microscope, it probably does not extend to the lower protective coating.

As a final example of the analysis of undercutting sites obtainable using microscopy, figure 12 presents an ensemble of views of a typical large pin-window site on sample AE, which was subject only to thermal AO. On this portion of the sample, the SiO_x film has been removed, a coating of Pt applied, and it has been mounted to a holder using black carbon tape.

Figure 12(a) shows this pin-window site on AE at a magnification of 500x at a single focal distance, which is satisfactory for planar measurements. Figure 12(b) shows the site at a magnification of 2000x, again using a single focal distance. The perspective view shown in figure 12(c) is constructed from a sequence of images taken at 2000x. This provides a complete view of the

cavity. The width of the cavity is 100 μm at the top and 36 μm at the bottom. The depth profiling analysis shown in figure 12(d) indicates a depth of 28.2 μm, which is about 11 percent greater than the 25.4 μm film thickness. The profile indicates that the cavity wall is irregular and slopes gradually to the lower coating. Although not necessarily visible at the small scale used for this figure, distinct demarcations exist around the lower periphery allowing identification of the wall edge and cavity bottom, which is now comprised of black carbon mounting tape and remnants of the lower SiO_x protective coating.

In general, the analysis obtained from examining individual undercutting sites was found to be consistent with the mass loss analysis and global coverage analysis. The overall analysis clearly points to thermal AO as being a more aggressive undercutting agent than hyperthermal AO when each is normalized with respect to erosion of witness material. The results of this study should prove useful in predicting erosion for polymers exposed to in-space AO.

The analysis of undercutting size and shape provided by this study provide useful information for calibrating numerical codes, which must rely on experimental results to fine tune erosion parameters. However, since the extent of undercutting is greatly influenced by the level of AO exposure, additional studies, including larger numbers of samples, are needed to adequately predict undercutting for arbitrary exposures. In particular, further analysis is needed to determine the size and distribution of defects and the dependence of undercutting on defect size.

4. Summary and Conclusion

This paper examined the effect of AO degradation of SiO_x protected Kapton H film due to AO undercutting erosion below generic defects in the protective coating. The effort was conducted at NASA GRC as part of MISSE 2 which was exposed to the LEO environment for approximately four years. The investigations for this paper focused on two flight samples exposed to in-space hyperthermal ram AO, but also included three non-flight samples. One flight sample was pristine before flight, but the other flight sample (as well as the non-flight samples) was pre-exposed to ground-based thermal AO. The thermal AO was equivalent to almost two years of in-space exposure based on Kapton H witness mass loss. It was produced using a isotropic RF plasma asher. Mass loss analysis and optical/electron microscopy analysis were conducted to determine changes in film characteristics resulting from AO exposure.

Analysis of mass loss revealed that the rate of mass loss with effective AO fluence is lower for hyperthermal exposure as compared to thermal exposure. In addition it was found that the rate of in-space erosion is substantially lower for protected film that has not been pre-exposed to thermal AO. This conclusion was supported by coarse and fine microscopy analysis. Global analysis of the samples revealed that the thermal AO exposure, even though it was substantially lower than the hyperthermal exposure, produced undercut cavities whose combined surface area comprised a much larger percentage of the sample surface than was the case for hyperthermal AO exposure. Analysis of typical individual sites using optical and electron microscopy revealed that the extent of undercutting due to hyperthermal AO was significantly less than that for thermal AO. Typical undercutting sites produced using thermal AO were much larger than the typical sites produced by hyperthermal AO even though the effective fluence was less than half that of the in-space case. It is concluded that thermal AO is an enhanced undercutting agent compared to hyperthermal AO when each is normalized with respect to erosion of witness material.

The results of this study should prove useful in predicting the AO durability of existing polymers and the new polymers that are candidates for the next generation of spacecraft materials.

References

1. de Groh K., et al. “Analyses of the MISSE PEACE Polymers International Space Station Exposure Experiment,” *Proc. ‘10th Symposium on Materials in a Space Environment*, Collioure, France 19–23 June 2006 (ESA SP–616).
2. Dever J.A., et al. “Effects of the Space Environment on Polymer Film Materials Exposed on the Materials International Space Station Experiment (MISSE 1 and MISSE 2),” Collioure, France 19–23 June 2006 (ESA SP–616).
3. Banks, B.A., et al. “Atomic Oxygen Erosion Phenomena,” American Inst. of Aeronautics and Astronautics Defense and Space Programs Conf., Huntsville, Al, Sept. 1997.
4. Banks, B.A., et al. “Monte-Carlo Computational Modeling of the Energy Dependence of Atomic Oxygen Undercutting of Protected Polymers,” Fourth International Space Conf. ICPMSE–4, Toronto, April 1998.
5. Snyder A., et al. “Fast Three-Dimensional Modeling of Atomic Oxygen Undercutting of Protected Polymers,” Journal of Spacecraft and Rockets, vol. 41, no. 2, May-June 2004.
6. Banks B.A., et al. “Atomic Oxygen Interaction with Solar Array Blankets at protective Coating Defect Sites,” 4th Annual Workshop on Space Operations, Automation and Robotics (*SOAR 90*), NM, June 1990.
7. Snyder A., “Investigation of Atomic Oxygen Erosion of Polyimide Kapton H Exposed to a Plasma asher Environment,” presented at the 44th International SAMPE Symposium and Exhibit, Long Beach, Calf., May 1999.
8. Snyder A., et al. “The Dependence of Atomic Oxygen Undercutting of Protected Polyimide Kapton H upon Defect Size,” *Proc. ‘8th Symposium on Materials in a Space Environment*, Arcachon, France, June 2000.

REPORT DOCUMENTATION PAGE

Form Approved
OMB No. 0704-0188

1. AGENCY USE ONLY (*Leave blank*)	2. REPORT DATE	3. REPORT TYPE AND DATES COVERED
	August 2006	Technical Memorandum

4. TITLE AND SUBTITLE

Undercutting Studies of Protected Kapton® H Exposed to In-Space and Ground-Based Atomic Oxygen

5. FUNDING NUMBERS

WBS 843515.01.15.03

6. AUTHOR(S)

Aaron Snyder, Bruce A. Banks, and Deborah L. Waters

7. PERFORMING ORGANIZATION NAME(S) AND ADDRESS(ES)

National Aeronautics and Space Administration
John H. Glenn Research Center at Lewis Field
Cleveland, Ohio 44135–3191

8. PERFORMING ORGANIZATION REPORT NUMBER

E–15665

9. SPONSORING/MONITORING AGENCY NAME(S) AND ADDRESS(ES)

National Aeronautics and Space Administration
Washington, DC 20546–0001

10. SPONSORING/MONITORING AGENCY REPORT NUMBER

NASA TM—2006-214387

11. SUPPLEMENTARY NOTES

Prepared for the 10th International Symposium on Materials in a Space Environment (ISMSE) cosponsored by the ONERA, CNES, and ESA, Collioure, France, June 19–23, 2006. Aaron Snyder and Bruce A. Banks, Glenn Research Center; Deborah L. Waters, QSS Group, Inc., 21000 Brookpark Rd., Cleveland, Ohio 44135. Responsible person, Aaron Snyder, organization code RPY, 216–433–5918.

12a. DISTRIBUTION/AVAILABILITY STATEMENT

Unclassified - Unlimited
Subject Categories: 23 and 27

Available electronically at http://gltrs.grc.nasa.gov

This publication is available from the NASA Center for AeroSpace Information, 301–621–0390.

12b. DISTRIBUTION CODE

13. ABSTRACT ***(Maximum 200 words)***

This study is part of a Materials International Space Station Experiment (MISSE) sequence to characterize the performance of prospective spacecraft materials when subjected to the synergistic effects of the space environment. Atomic oxygen (AO) is the most prevalent species in low earth orbit (LEO). In this environment AO is mainly responsible for the erosion of hydrocarbons and halocarbon polymers. The AO erosion rates of Kapton (DuPont) H are known and well documented. Hence, it is customary to compare the AO erosion yields of candidate materials to the commonly accepted standard of this polyimide. The purpose of this study was to provide characterization of AO degradation of SiO_x protected Kapton H film, which was subject during MISSE 2 to undercutting erosion beneath microscopic defects in the protective film, and compare the degradation resulting from hyperthermal ram (~4.5 eV) LEO AO to the degradation resulting from exposure to thermal ground-based (~0.04 eV) AO.

14. SUBJECT TERMS	15. NUMBER OF PAGES
Earth orbital environment; Polymer degradation; Atomic oxygen	13
	16. PRICE CODE

17. SECURITY CLASSIFICATION OF REPORT	18. SECURITY CLASSIFICATION OF THIS PAGE	19. SECURITY CLASSIFICATION OF ABSTRACT	20. LIMITATION OF ABSTRACT
Unclassified	Unclassified	Unclassified	